Advanced Multivariable Control of a Pilot-Plant Distillation Column

This paper reports an experimental study of the multivariable control of a pilot-plant distillation column having a side stream as well as overhead and bottom products. A recently developed multivariable controller for systems having multiple time delays is implemented for the first time on an experimental process. The controller consists of a new multivariable time delay compensator coupled with traditional PI controllers. Realization is accomplished with a PDP 11 minicomputer. Improved system performance was observed with the delay compensator, especially in disturbance rejection.

B. A. OGUNNAIKE, J. P. LEMAIRE, M. MORARI, and W. H. RAY

Department of Chemical Engineering
University of Wisconsin
Madison, WI 53706

SCOPE

Multivariable systems having multiple time delays are often difficult to control effectively using traditional single loop controllers. A multidelay compensator (Ogunnaike and Ray, 1979), developed to address this problem, has been shown to work well through simulation on various test problems.

In the present work, we report an experimental application of this multidelay compensator to pilot-scale distillation column control. The performance of a multiproduct ethanol-water, pilot-plant distillation column (modelled by a 3×3 transfer function matrix) under traditional single-loop PI control is compared with performance when the multidelay compensator is incorporated.

This investigation constitutes the first experimental test of the recently developed control strategy.

CONCLUSIONS AND SIGNIFICANCE

Overall, the control scheme incorporating the multidelay compensator performed better than the traditional single-loop PI controllers, especially in disturbance rejection. This performance of the delay compensator carried over into experimental tests under conditions in which the system's mathematical model was no longer adequate—thus establishing the robustness of this control strategy.

It is expected that in industrial scale columns, where system delays will be considerably larger, even greater advantage over traditional PI controllers than observed in this investigation can be expected.

INTRODUCTION

Industrial users consume more than one fourth of the total energy used in the U.S. [10.3 million out of some 40 million bbl (6 million m^3) of oil (equivalent) per day]. It is estimated (Brookhaven National Laboratory Report, 1978) that almost half of this energy [4.6 million bbl (0.7 million m^3)] is unrecovered and thus lost. Though some of these losses are unavoidable, the economic incentives for more efficient process design and operation are significant. We cite a few examples:

- It was estimated that if the energy efficiency of distillation, one of the most important separation operations in the process industries, were increased by 10%, a savings of 100,000 bbl (16,000 m^3) of oil/day would result in the U.S. alone (cf. Mix et al., 1977). This amounts to a savings in imports of about $500 million/yr at current prices.
- Retrofitting and improved energy integration of multicomponent distillation trains have been demonstrated to reduce the energy consumption by as much as 40% (Freshwater and Ziogou, 1976).

A realistic engineering approach to the solution of energy efficiency problems in the process industries has to proceed in parallel along the following two lines:

1) The development of improved process designs with energy efficiency as a primary objective.

2) The development of new process control strategies to allow these new energy-integrated processes to operate in a reliable and safe manner in the face of varying raw material quality, product specifications, process upsets, etc.

There is at present a great deal of effort both in industry and at universities directed toward more energy-efficient process designs. However, there seems to be relatively little fundamental work directed toward the solution of the more complex process control problems resulting from the great energy integration and complex dynamic interactions in these new designs. This dynamic aspect of energy efficiency is particularly important because of the dramatic changes in computer technology over the last ten years which allow routine realization of sophisticated process control algorithms at low cost.

The present paper is devoted to one aspect of this important industrial control problem—the testing of newly developed multivariable control strategies on a multiproduct distillation column having interactions between control loops and multiple time delays. This is the first experimental test of our recently developed multivariable control strategy.

B. A. Ogunnaike is on leave from Department of Chemical Engineering, University of Lagos, Lagos, Nigeria. He is presently with Shell Development Co., Houston, TX.
J. P. Lemaire is presently with Rhone-Poulenc, Fontenoy, France.
Correspondence concerning this paper should be addressed to W. H. Ray.

MULTIVARIABLE CONTROL ALGORITHM

Recently, Ogunnaike and Ray (1979) developed a multidelay compensator which, in the absence of model error, removes all time delays from the closed loop characteristic equation. The compensator, which can handle state, output, or input delays, has been tested through simulation on a number of test problems (Ogunnaike and Ray, 1979, 1982) and found to work well. In addition, a general purpose computer-aided design program (Ogunnaike and Ray, 1982), has been developed which allows the compensator to be integrated into an overall multivariable design strategy.

Although this multivariable control strategy may be implemented for either time domain or Laplace transform models, here we shall outline the essential features using a Laplace domain model. For multivariable systems such as distillation columns having multiple delays, a commonly employed linear model takes the form

$$\boldsymbol{y}(s) = \boldsymbol{G}(s)\boldsymbol{u}(s) + \boldsymbol{G}_d(s)\boldsymbol{d}(s) \tag{1}$$

where $\boldsymbol{y}$ is a vector of outputs, $\boldsymbol{u}$ a vector of controls, and $\boldsymbol{d}$ a vector of disturbance variables. The transfer functions $\boldsymbol{G}(s)$, $\boldsymbol{G}_d(s)$ have the general form:

$$\boldsymbol{G}(s) = \begin{bmatrix} g_{11}(s) & g_{12}(s) & \cdots & g_{1m}(s) \\ g_{12}(s) & & & \\ & \ddots & & \\ g_{l1}(s) & & & g_{lm}(s) \end{bmatrix}; \qquad \boldsymbol{G}_d(s) = \begin{bmatrix} g^d_{11}(s) & g^d_{12}(s) & \cdots & g^d_{1k}(s) \\ g^d_{12}(s) & & & \\ & \ddots & & \\ g^d_{l1}(s) & & & g^d_{lk}(s) \end{bmatrix} \tag{2}$$

where the elements $g_{ij}(s)$, $g_{ij}{}^d(s)$ both have the form

$$g_{ij}(s) = \frac{k_{ij} \prod_{p=1}^{n} (e_{ijp}s + 1)e^{-\alpha_{ij}s}}{\prod_{q=1}^{r} (f_{ijq}s + 1)} \tag{3}$$

where:

r = order of the transfer function
n = number of zeroes ($n \leq r$)
$-(e_{ijp})^{-1}$ = zeroes of the transfer function, g_{ij}
$-(f_{ijq})^{-1}$ = poles of the transfer function, g_{ij}
k_{ij} = steady state gain of g_{ij}
α_{ij} = time delay associated with g_{ij}

As noted above, our research group has developed a multidelay compensator which applies for multivariable systems having any number of time delays (Ogunnaike and Ray, 1979). The structure of the multidelay compensator is shown in Figure 1, where G_K is the compensator and G_c the conventional controllers. If one chooses

$$G_K = G^*(s) - G(s) \tag{4}$$

where $G^*(s)$ is the process transfer function without time delays, the time delays are totally eliminated from the closed loop characteristic equation. This, of course, allows much larger controller gains to be used. The improvement in control system performance due to this compensator, as determined by simulation, was found to be significant for chemical reactor trains with delayed recycle and for distillation columns (Ogunnaike and Ray, 1979).

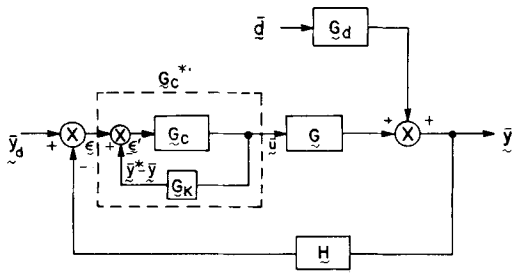

Figure 1. Block diagram for the feedback control of a multi-variable system using the multidelay compensator.

This new multivariable control strategy is formulated in such a way that it can be integrated with interaction compensation methods. As has been shown in Ogunnaike and Ray (1982), it allows loop interactions to be handled with more conventional multivariable control design procedures (such as noninteracting control, characteristic loci methods, Nyquist array approaches). This new methodology has been implemented on the distillation column described in the next section.

DISTILLATION COLUMN

Although the multivariable control strategy described in the previous section has worked well in simulation, the theoretical basis of the design assumes perfect modelling of the process to be controlled. Thus, a realistic test of the control system performance must involve experimental studies on a process for which only approximate process models are available (a common situation in industrial practice). In the present paper, we report results for the control of a multi-product pilot plant distillation column using this new control algorithm.

The distillation column studied was a 19 plate, 12 inch diameter copper column having variable feed and side stream draw-off locations. Temperatures were measured on each tray as well as in the overhead, reflux, feed, and product lines. Compositions may be determined through various on-line sensors (densitometry, refractometry, etc.). Data acquisition and computer control were carried out through interfacing to a PDP 11/55 minicomputer. A schematic diagram of the column is shown in Figure 2. The present study was concerned with the binary ethanol-water system, but later results will include ternary mixtures.

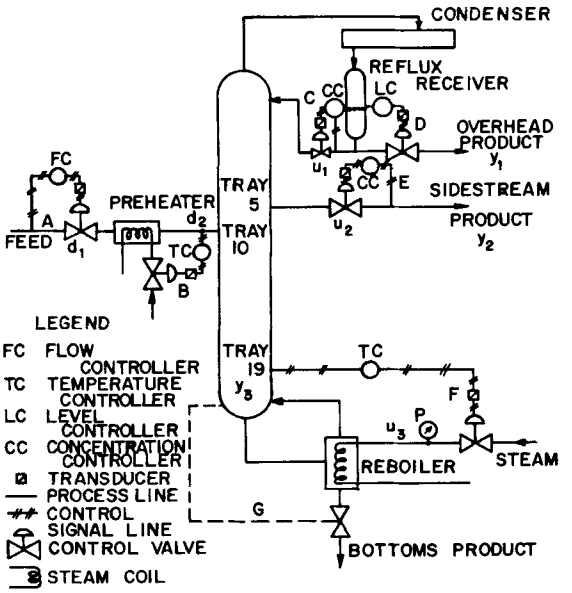

Figure 2. Schematic diagram of the experimental distillation column.

RESULTS

Process Model

A model relating outputs to inputs and disturbances has been determined through pulse testing of the column and fitting of simple first-order-plus delay transfer functions to most elements of the process model (1–3), and in some cases some slightly more complicated forms.

For the binary ethanol-water system, the column model takes the form of Eq. 1 where the outputs are

y_1 = overhead ethanol mole fraction

y_2 = side stream ethanol mole fraction

y_3 = tray #19 temperature, °C (corresponding to bottoms composition)

The inputs (Appendices B and C) are

u_1 = reflux flow rate, gpm (m^3/s)

u_2 = side stream product flow rate, gpm (m^3/s)

u_3 = reboiler stream pressure, psig (kPa)

and the disturbances (Appendices B and C) are

d_1 = feed flow rate, gpm (m^3/s)

d_2 = feed temperature, °C

The experimentally obtained model is shown in Table 1. Figures 3 and 4 show experimental data from two-pulse tests and the resulting transfer function model fits of the data. Parameters were estimated by regular least squares in the frequency domain and by direct minimization of the sum of squares surface (on the data in the time domain) using a standard optimization routine (cf. Lemaire, 1980; Ogunnaike, 1981).

TABLE 1. DISTILLATION COLUMN MODEL

$$y(s) = G(s)u(s) + G_d(s)d(s).$$

$$G(s) = \begin{bmatrix} \frac{0.66e^{-2.6s}}{(6.7s+1)} & \frac{-0.61e^{-3.5s}}{(8.64s+1)} & \frac{-0.0049e^{-s}}{(9.06s+1)} \\ \frac{1.11e^{-6.5s}}{(3.25s+1)} & \frac{-2.36e^{-3s}}{(5.0s+1)} & \frac{-0.012e^{-1.2s}}{(7.09s+1)} \\ \frac{-34.68e^{-9.2s}}{(8.15s+1)} & \frac{46.2e^{-9.4s}}{(10.9s+1)} & \frac{0.87(11.61s+1)e^{-s}}{(3.89s+1)(18.8s+1)} \end{bmatrix}$$

$$G_d(s) = \begin{bmatrix} \frac{0.14e^{-12s}}{(6.2s+1)} & \frac{-0.0011(26.32s+1)e^{-2.66s}}{(7.85s+1)(14.63s+1)} \\ \frac{0.53e^{-10.5s}}{(6.9s+1)} & \frac{-0.0032(19.62s+1)e^{-3.44s}}{(7.29s+1)(8.94s+1)} \\ \frac{-11.54e^{-0.6s}}{(7.01s+1)} & \frac{0.32e^{-2.6s}}{(7.76s+1)} \end{bmatrix}$$

Note: Time unit is minutes.

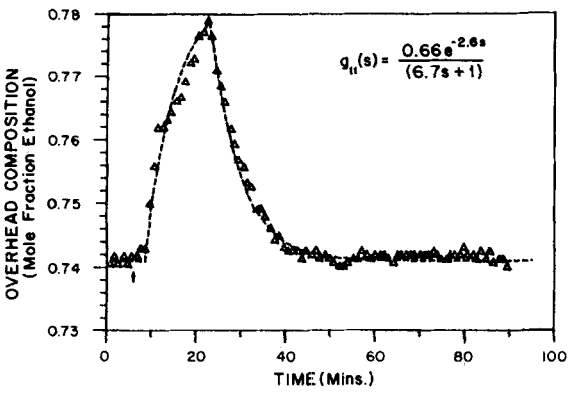

Figure 3. Overhead composition response to a pulse of 15 minutes duration in reflux rate (model vs. data).

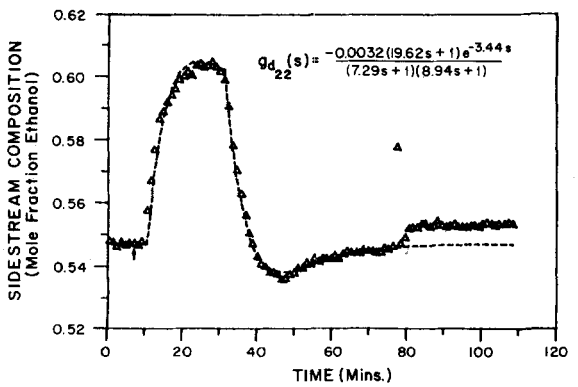

Figure 4. Side-stream composition response to a pulse of 15 minutes duration in feed temperature (model vs. data).

Control System Development

The implementation of our control scheme requires real time computer realization of the delay compensator. With the aid of the CAD program discussed in Ogunnaike and Ray (1982), the differential equations representing the delay compensator were obtained as shown in part I of Appendix A. Because of the nature of these equations, analytical solutions readily exist. When the inputs $u(t)$ are constant over a period of time Δt (as is the case with our DDC system), the analytical solutions to the compensator equations become the algebraic equations in part II of Appendix A. These are the equations used in the control study to implement the delay compensator.

The determination of controller settings to use for multi-variable systems still remains a problem with no universally acceptable solution. In our case, dynamic simulations of the control system (using the CAD program of Ogunnaike and Ray, 1982) were used

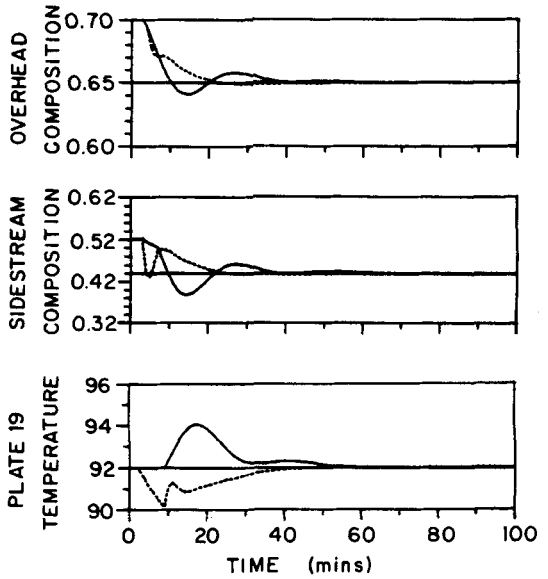

Figure 5. Simulated expected system response to set point changes. - - - - - with the delay compensator; —— without the delay compensator

TABLE 2. BEST CONTROLLER SETTINGS*

Control Strategy \ Control Loop	Overhead K_c	Overhead $1/\tau_I$	Side Stream K_c	Side Stream $1/\tau_I$	Bottoms Temperature K_c	Bottoms Temperature $1/\tau_I$
PI + Delay Compensator	1.2	0.333	−1.5	0.714	1.2	0.556
PI Alone	1.2	0.2	−0.15	0.1	0.6	0.25

* Obtained using system simulations.

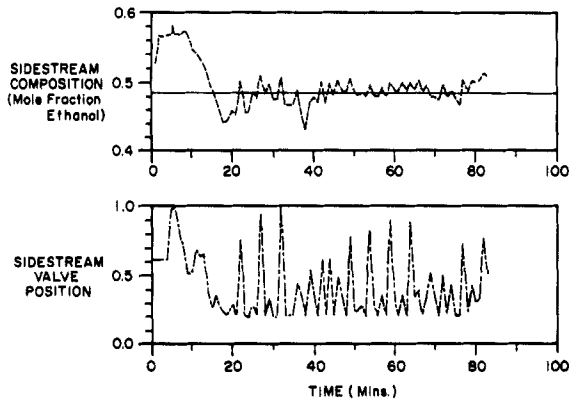

Figure 6. Noisy side stream composition readings and the effect on the side stream control valve.

to obtain controller parameters which gave the best control system response to set point changes for regular PI controllers with and without the time delay compensators (Figure 5). These values are displayed in Table 2.

In carrying out feedback control it was found that the side stream composition readings were very noisy, perhaps as a result of the shallowness of the trays. (The distillation column was not originally designed for continuous withdrawal of side stream products.) It was typical, for set point changes, to obtain such behavior as shown in the top half of Figure 6. With such erratic readings, the control valve position oscillates as shown in the bottom half of Figure 6. To eliminate this valve chatter, a first order digital filter was included in the real time program to take care of these rather unnatural fluctuations for all experimental runs. The filter equation used was

$$\hat{Y}_t = 0.8Y_t + 0.2\hat{Y}_{t-1}$$

where Y_t represents the current side stream composition measurement, and $\hat{Y}_t$ is the filtered measurement. Control action was taken at each time based on the filtered measurement.

Control System Evaluation

This section is devoted to critical discussions of the experimental results obtained during our computer control studies. In each of these experimental runs, the column was brought to steady state (Appendix B) and allowed to operate for a period of time before the system was perturbed either by set point changes or step changes in the disturbances. The graphical records of the subsequent system responses carry arrows which indicate at what instance the particular perturbation in question was introduced. In all of these graphs, the system behavior using the delay compensator is represented in dotted lines while the solid lines represent the behavior *without* the delay compensator.

Response to Set Point Changes. When the controllers operating with the parameters in Table 2 were implemented on the actual distillation column, the system response to a 5% and 8% decrease in the respective set points for the overhead and side stream compositions is shown in Figure 7. (Here it was desired to maintain the bottoms temperature at 92°C.) Note that with the overhead composition, the system starts out responding almost identically both with and without the time delay compensator, but ultimately, sustained oscillations arise under regular PI control while with the delay compensator the system attains the new steady state in less than 20 minutes of operation. The response of the side stream composition and bottoms temperature were also improved with the time delay compensator.

If we examine the controller settings in Table 2, we observe that, as expected, the time delay compensator permits the use of higher controller gains. When such high gains were used with the PI controller alone, the system went completely unstable.

Figure 5 shows the expected system response as predicted by the

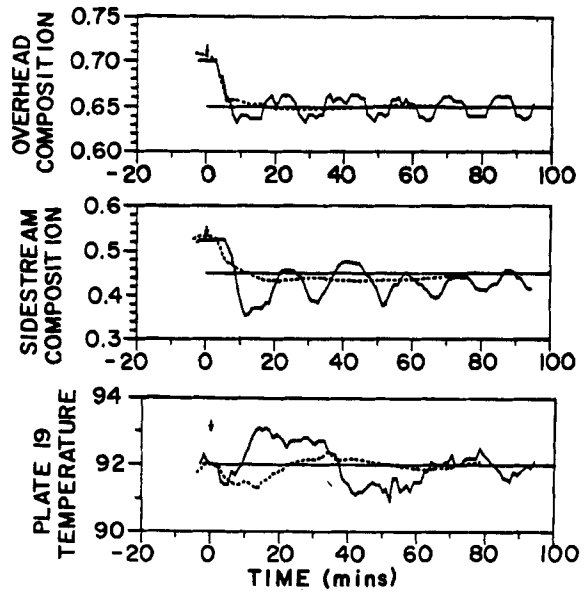

Figure 7. System response to set point changes in top products (Controller Settings of Table 2). - - - - - with the delay compensator; — without the delay compensator.

model, when the controller parameters in Table 2 are used. However, it appears from the experimental results (Figure 7) that the PI controller parameters need to be more conservative than predicted from simulation. Thus new controller settings shown in Table 3 were used for the PI controller and the resulting system response (superimposed on the previously shown response with the delay compensator) is shown in Figure 8. Note that the PI controller performance has improved considerably and there is reasonable qualitative agreement with the model predictions in Figure 5 (even though the controller parameters have had to be changed to achieve

TABLE 3. RETUNED SETTINGS FOR THE PI CONTROLLERS

	K_c	$1/\tau_I$
Overhead	0.6	0.2
Side Stream	−0.07	0.1
Bottoms	0.6	0.25

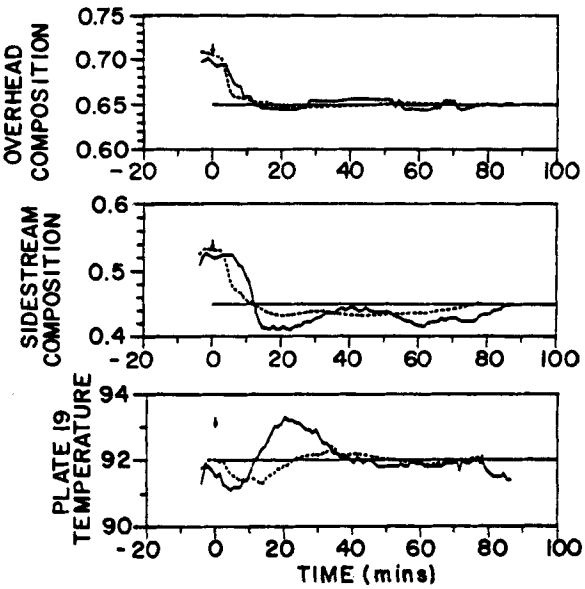

Figure 8. System response to set point changes in top products (Detuned PI controllers). - - - - - with the delay compensator; — without the delay compensator.

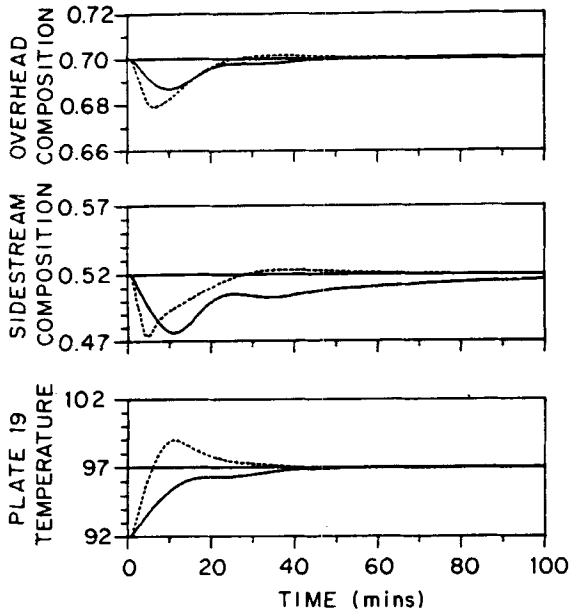

Figure 9. Simulated expected system response to a 5°C set point change in tray 19 temperature. - - - - - with the delay compensator; — without the delay compensator.

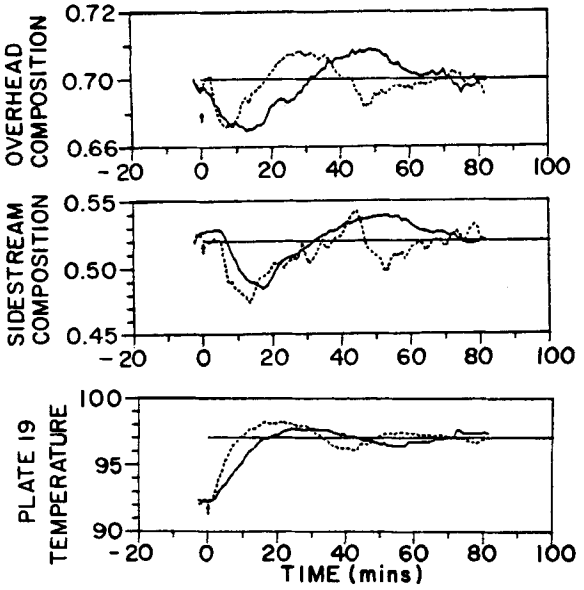

Figure 10. System response to a 5°C set point change in tray 19 temperature. - - - - - with the delay compensator; — without the delay compensator.

this). The performance using the delay compensator still remains somewhat better however.

A very important point to note in Figure 8 is that the advantage in using the compensator is more pronounced for the response of the tray #19 temperature. While there is still noticeable advantage in the side stream response, observe that the overhead response is only slightly better with the delay compensator than without. The model-based simulations in Figure 5, which do not suffer from the effect of modeling errors, predict the same trends. This suggests that one should not expect a greater advantage of the delay compensator over the regular PI controller than indicated in Figure 8 for set point changes.

The reason for this, we believe, could be seen from a close examination of the system model. From the structure of our time delay compensator block with $G_K = G^* - G$, the closer the system model G is to G^*, the closer G_K is to zero (where our technique reduces to regular PI control). The sampling interval for our control system being 1 min, we observe that the delays on the main diagonal of G (cf. Table 1) and on the upper triangular portion are no more than thrice the sampling time. Thus, in terms of delay compensation, the model indicates that with careful tuning (because some of the elements do not have very large delays), the regular PI controller could be made to perform almost as well as when the delay compensator is used. Nevertheless, the fact that there are still delays dictates that the delay compensator should still perform better; how much better is dependent on how large the time delays are.

A look at the lower triangular element of G however presents an entirely different picture. Although still not too large, these time delays are much larger than those on the main diagonal and on the upper triangular portion. The resulting effect is as follows. For *set point changes* in the overhead and side stream compositions, the principal reason the temperature on tray #19 departs from its steady state value (92°C) is because of the dynamic interactions which are represented by the $g_{31}(s)$ and $g_{32}(s)$ elements of $G(s)$. But observe that the delays involved with these are about nine times the sampling time. Hence even though the PI controller (without the compensator) strives to perform almost as well as the delay compensator does with the overhead composition control, the advantage of the delay compensator in the control of the temperature on tray 19 is significant.

In discussing the system response to *set point changes* in the third variable, tray #19 temperature, it is quite informative to first study the system model. All the elements of $G(s)$ which are of interest in this case are those occupying the third column. Observe that these are the elements having uniformly minimum time delays; hardly larger than *one* sampling time. The implications are that since there is not much delay to compensate for, no dramatic advantages should be expected from using the time delay compensator. To illustrate a 5°C set point change in the tray #19 temperature, a simulation of the expected system response is shown in Figure 9 for delay compensated and uncompensated PI control. (At the steady-state value of 92°C for T_{19}, the bottoms composition is about 99% H_2O. A 5°C set point change from 92 to 97°C corresponds to a bottoms composition change from 99 to 99.8% H_2O.) The only reason for significant differences between the two sets of responses is that the controller settings are different for the two controllers (Table 2).

It is, therefore, not surprising that the experimental results turned out as shown in Figure 10. The same parameter settings noted in Table 2 were used for the controllers operating with the delay compensator while the Table 3 parameters were used for the PI controllers *without* the compensator. (Fair qualitative agreements between the theoretical expectations and the experiments can be

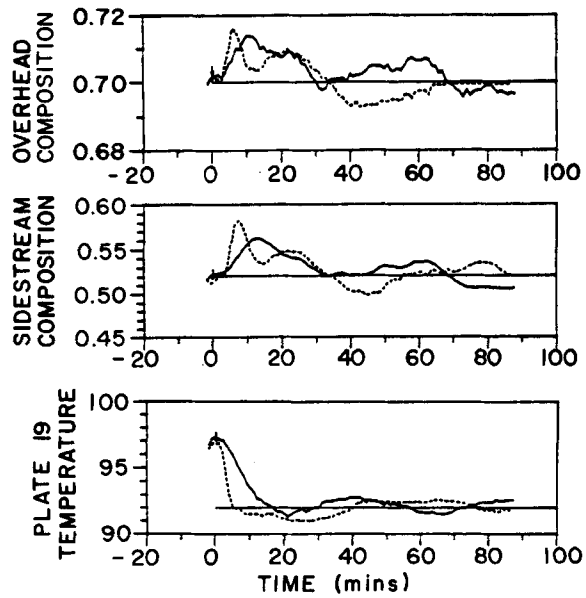

Figure 11. System response to a −5°C set point change in tray 19 temperature. - - - - - with the delay compensator; — without the delay compensator.

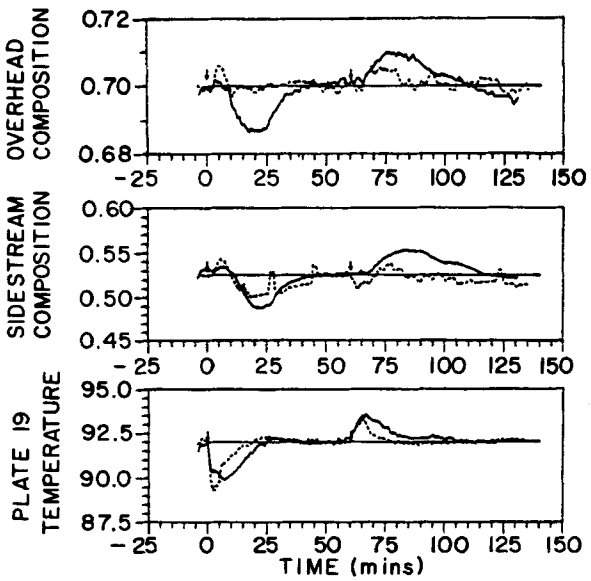

Figure 12. System response to disturbance in feed rate as shown. - - - - - with the delay compensator; — without the delay compensator.

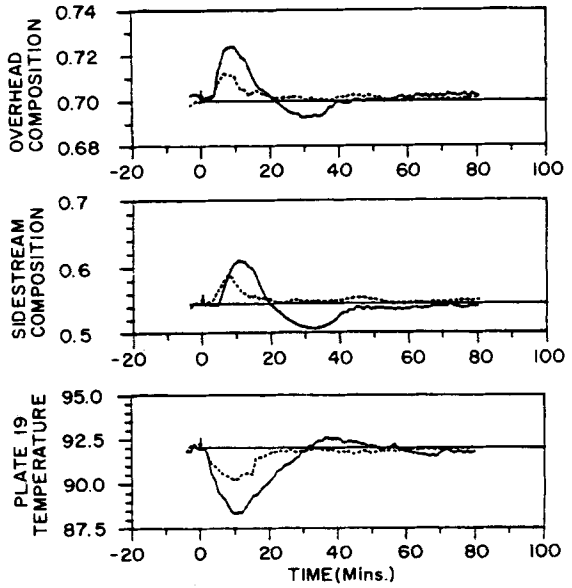

Figure 14. System response to a −20°C step disturbance in feed temperature. - - - - - with the delay compensator; — without the delay compensator.

seen by comparing Figures 9 and 10.) The advantage of speed of response is observed with the time delay compensator—especially for T_{19}, but overall performance is only marginally better.

A set point change in the opposite direction (from 97 back to 92°C) resulted in the response shown in Figure 11. It can be seen from here that the system is mildly nonlinear; otherwise, Figure 11 should have turned out approximately like a mirror image of Figure 10. The time delay compensated system performs in a slightly better fashion; the speed of response being much faster, but with comparable settling times.

From the above results on *set point changes*, we come to the conclusion that using the time delay compensator results in slightly better system performance, but the advantages are not very dramatic as a result of the nature of the system.

Response to Step Changes in Disturbance Variables. After having studied the control system performances under set point changes, the next investigations centered on the disturbance rejection capabilities. Once a control system has been designed, it is usually expected to perform both disturbance rejection and reasonable set point response. Thus it was decided to test the disturbance rejection

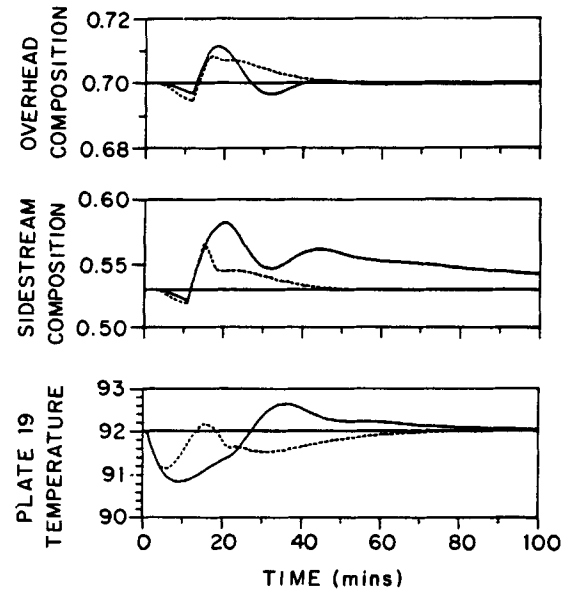

Figure 13. Simulated expected system response to a step up in the feed rate. - - - - - with the delay compensator; — without the delay compensator.

of the control systems while operating with the same parameters as those used in the previous study on set point changes (i.e., parameters in Table 2 for PI control *with* delay compensation, and those in Table 3 for PI control *without* compensation). As in the last discussion, all the graphical records of the system responses are recorded in dotted lines for the delay compensated system and in solid lines for the uncompensated system.

Figure 12 shows the response to a feed rate disturbance. From the usual steady state value of 0.8 gpm (0.05 L/s), the feed rate was changed to 1 gpm (0.06 L/s) and held at this value for 1 hour, after which it was returned to its previous value. The arrows in Figure 12 indicate when the feed rate was changed in each instance.

Here, performance with the delay compensator is seen to be markedly better as the dotted lines show. (The side stream performance might have been affected by the two obviously spurious composition readings which show up around t = 28 min and t = 45 min as spikes.) The fact that the two portions of each set of graphs do not exactly look like mirror images is another indication of the nonlinearities inherent in the system. The simulated expected system response for the first half of the disturbance [i.e., the step up from 0.8 gpm (0.05 L/s) to 1 gpm (0.06 L/s)] is shown in Figure 13.

The clearly better disturbance rejection capabilities obtained with the delay compensator is not limited only to feed rate disturbances. The system response to a 20°C drop in the feed temperature (from 78 to 58°C) is shown in Figure 14 where the performance with the delay compensator is seen to be much better than without. The simulated expected system response shown in Figure 15 also qualitatively agrees with the experimental results.

If we again examine the system model, this time $G_d(s)$, the disturbance transfer function matrix (recall that this information is not built into the delay compensator block), we find that there are some interesting features which we believe have some bearing on the performance of the delay compensator in disturbance rejection. Especially for the feed rate disturbance, the elements of G_d in the first column (which represent the effect of feed rate on the three system variables) carry delay factors which are not only large, but cover a wide span, from ½ min to 12 min. The implication is that the system feels the disturbance at three separate times. The temperature T_{19} feels the effect first; owing to interactions, the overhead and side stream products start to respond also. But these will, in approximately 9 minutes, return to affect the temperature. Just when the system is getting adjusted to the disruption, the side stream starts to respond to the original feed disturbance, setting off its own series of disruptions approximately as indicated

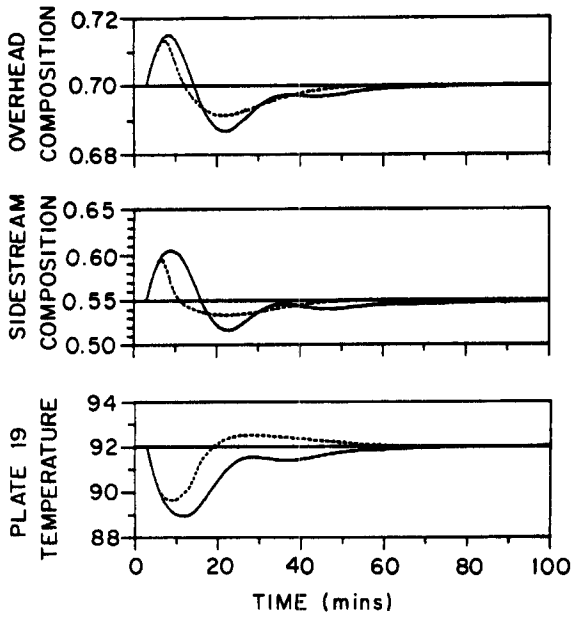

Figure 15. Simulated expected system response to a −20°C step disturbance in feed temperature. - - - - - with the delay compensator; —— without the delay compensator.

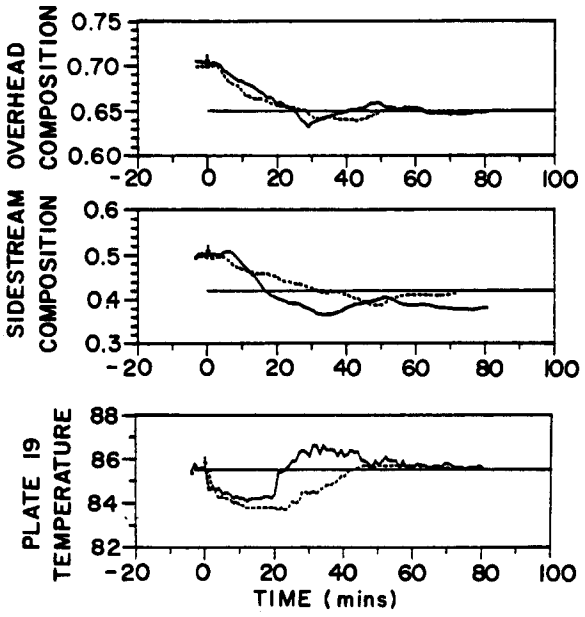

Figure 16. System response to set point changes in top products under drastically altered operating conditions. - - - - - with the delay compensator; —— without the delay compensator.

by $G(s)$. It will not be until 12 minutes after the feed disturbance was implemented that the overhead product starts to react directly to this disturbance, while in addition setting off yet another series of additional disruptions in a fashion approximated by $G(s)$.

The delay compensated system has the expected system behavior contained in $G(s)$ built into its structure. No matter how imperfect this knowledge, it aids the controller in that it provides information about how the system will react to all the secondary and higher order disruptions when they do start occurring. It, therefore, performs better than the regular, uncompensated PI controllers which have to react with no such background knowledge.

Although improvements in the control system performance could have been made by implementing interaction compensators for the time-delay compensated system, this was not carried out. Instead we embarked on experimental studies on the robustness of the delay compensator. Because this technique is so dependent on the system model, questions of robustness in the face of modeling errors are of great importance. To study this, we carried out experiments as greatly altered feed concentrations without adjusting the system model.

When the feed is charged from a 6% ethanol-water mixture to one containing 20% ethanol (more than 300% increase!) while keeping the reflux and side stream flow rates as well as the steam pressure at their usual values of 0.18 gpm (0.01 L/s), 0.046 gpm (0.003 L/s, and 20 psig (138 kPa), respectively, the results are:

(i) The reflux ratio (at steady state) drops from 3 to about 1.5.

(ii) The overhead composition at steady state still remains at 70% ethanol, but the side stream composition becomes 50% ethanol (from 53%) and the tray #19 temperature drops to 85°C from 92°C; corresponding to a bottoms composition increase from 1% ethanol to about 10%.

When the usual 5 and 8% set point changes are made in the overhead and side stream compositions respectively, the control system (just as it was set up for all the runs hitherto discussed) responded as shown in Figure 16. Clearly the responses are a little more sluggish but it is interesting to note the consistency in how the delay compensated system compares with the uncompensated system (cf. Figure 8). As in the earlier studies, both controllers respond about equally well to set point changes.

To illustrate the performance under disturbances, the response to a step change in the feed rate from 0.8 to 1 gpm (0.05 to 0.06 L/s) as a disturbance was also studied. Since the delay compensator previously had performed very well, it is useful to see its perfor-

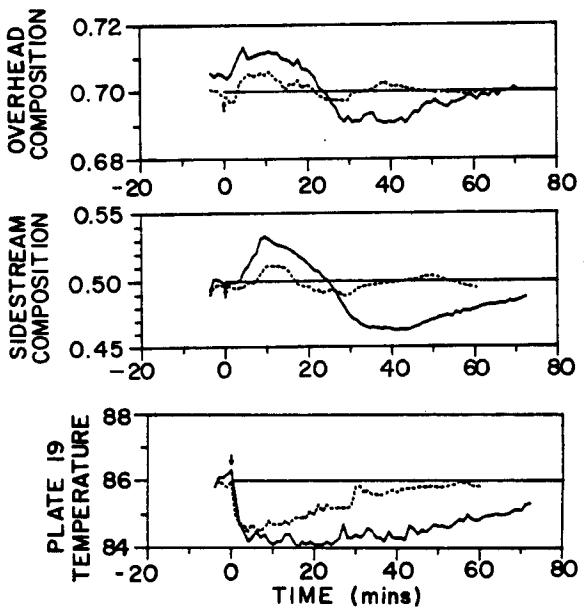

Figure 17. System response to a 20% step up in feed rate under drastically altered operating conditions. - - - - - with the delay compensator; —— without the delay compensator.

mance when the model can no longer be considered very accurate. The system response is shown in Figure 17 where we notice that the performance with the delay compensator still remains considerably better than the response without it. In fact this robustness of the multivariable time delay compensator, both in simulation (cf. Ogunnaike and Ray, 1982) and under experimental conditions is a pleasant surprise given the experience with single loop Smith predictors. Work is under way to adequately explain this unusually good performance.

ACKNOWLEDGMENTS

We are pleased to acknowledge the technical support and help we received from Todd Ninman, Don Zentner and Norman Jerome. We are also indebted to Bruce Bal, Connie Kieckhefer, and Brian Strothmann who were invaluable as undergraduate research

assistants. We are indebted to the National Science Foundation, the Department of Energy, and to Exxon for financial support. B. A. Ogunnaike has been supported by the Department of Chemical Engineering, University of Lagos, during his graduate study.

NOTATION

A	= state vector matrix coefficient in state-space realization
B_j	= control vector matrix coefficient in state-space realization
C	= output matrix coefficient
G, G_d, G_K, G^*	= transfer function matrices
g_{ij}, g^d_{ij}	= elements of transfer function matrices
H	= measurement transfer function
K_c	= proportional controller gain
s	= Laplace operator
T_{19}	= temperature on tray #19
u	= control vector
w	= compensator block output vector
y	= system output
$\hat{Y}_t$	= filtered measurement
z	= state vector of the compensator equations

Greek Letters

β_j	= time delay in control path
Δt	= DDC sampling interval
θ	= dummy time argument
τ_I	= integral time

Superscripts

*	= multidelay compensator quantities
^	= filtered quantities

Subscripts

ov	= overhead
ss	= side stream

APPENDIX A

Part I. Compensator Equations

$$\dot{z}_1 = -0.1492\, z_1 + 0.0984\,[u_1(t) - u_1(t-2.6)]$$
$$\dot{z}_2 = -0.1157\, z_2 - 0.0708\,[u_2(t) - u_2(t-3.5)]$$
$$\dot{z}_3 = -0.1103\, z_3 - 0.0005\,[u_3(t) - u_3(t-1)]$$
$$\dot{z}_4 = -0.3074\, z_4 + 0.3412\,[u_1(t) - u_1(t-6.5)]$$
$$\dot{z}_5 = -0.2002\, z_5 - 0.4718\,[u_2(t) - u_2(t-3.0)] \qquad \text{(A1)}$$
$$\dot{z}_6 = -0.1281\, z_6 - 0.0015\,[u_3(t) - u_3(t-1.2)]$$
$$\dot{z}_7 = -0.1227\, z_7 - 4.2552\,[u_1(t) - u_1(t-9.2)]$$
$$\dot{z}_8 = -0.0917\, z_8 + 4.2385\,[u_2(t) - u_2(t-9.4)]$$
$$\dot{z}_9 = -0.2571\, z_9 + 0.1157\,[u_3(t) - u_3(t-1)]$$
$$\dot{z}_{10} = -0.0532\, z_{10} + 0.0223\,[u_3(t) - u_3(t-1)]$$

with

$$\left.\begin{aligned} w_1 &= z_1 + z_2 + z_3 \\ w_2 &= z_4 + z_5 + z_6 \\ w_3 &= z_7 + z_8 + z_9 + z_{10} \end{aligned}\right\} \qquad \text{(A2)}$$

This could be written more compactly as

$$\dot{\boldsymbol{z}} = \boldsymbol{A}\boldsymbol{z} + \sum \boldsymbol{B}_j[\boldsymbol{u}(t) - \boldsymbol{u}(t-\beta_j)] \qquad \text{(A3)}$$

$$\boldsymbol{w} = \boldsymbol{C}\boldsymbol{z} \qquad \text{(A4)}$$

where the elements of each of the matrices are obvious from the above full representation.

In terms of the variables in Figure 1, $\boldsymbol{w} = \boldsymbol{y}^* - \boldsymbol{y}$.

Part II. Compensator Equation As Implemented in DDC

The analytical solution to Eq. A3 can be readily shown to be

$$\boldsymbol{x}(t) = e^{\boldsymbol{A}t}\boldsymbol{x}_0 + \int_0^t e^{\boldsymbol{A}(t-\theta)} \left\{ \sum_j \boldsymbol{B}_j[\boldsymbol{u}(\theta) - \boldsymbol{u}(\theta - \beta_j)] \right\} d\theta$$

Considering $\boldsymbol{u}(t)$ as constant between t and $t + \Delta t$ (as is the case with DDC) we have

$$\boldsymbol{x}(t + \Delta t) = \boldsymbol{\Phi}\boldsymbol{x}(t) + \sum_j \boldsymbol{\psi}_j[\boldsymbol{u}(t) - \boldsymbol{u}(t - \beta_j)] \qquad \text{(A5)}$$

where

$$\boldsymbol{\Phi} = e^{\boldsymbol{A}\Delta t}$$
$$\boldsymbol{\psi}_j = \boldsymbol{A}^{-1}[\boldsymbol{\Phi} - \boldsymbol{I}]\boldsymbol{B}_j \qquad \text{(A6)}$$

Thus given $\boldsymbol{x}(n)$ and $\boldsymbol{u}(n)$ (and the previous controls) for the sampling instant n, the delay compensator is implemented for our system by

$$\boldsymbol{x}(n+1) = \boldsymbol{\Phi}\boldsymbol{x}(n) + \sum_j \boldsymbol{\psi}_j[\boldsymbol{u}(n) - \boldsymbol{u}(n - \beta_j)] \qquad \text{(A7)}$$
$$\boldsymbol{w}(n+1) = \boldsymbol{C}\boldsymbol{x}(n+1)$$

where the matrices are defined in Eq. A6 with the numerical values for $\boldsymbol{A}$, $\boldsymbol{B}_j$, and $\boldsymbol{C}$ as shown in Part I.

APPENDIX B

I. Table of Usual System Steady-State Values

Control Variables		Controlled Variables	
Reflux Flow Rate	0.18 gpm (0.01 L/s)	Overhead Mole Fraction Ethanol	0.7
Side Stream Flow Rate	0.046 gpm (0.003 L/s)	Side Stream Mole Fraction Ethanol	0.52
Reboiler Steam Pressure	20 psig (137.89 kPa)	Temperature on Tray #19	92°C

II. Table of System Constraints

	Lower Constraint	Upper Constraint
Reflux Flow Rate	0.068 gpm (0.004 (L/s)	0.245 gpm (0.02 L/s)
Side Stream Flow Rate	0.00694 gpm (0.00044 L/s)	0.1 gpm (0.01 L/s)
Reboiler Steam Pressure	15.6 psig (107.56 kPa)	34.0 psig (234.42 kPa)

APPENDIX C

TABLE OF EXPERIMENTAL RUNS

Run #	Experimental Conditions: Experiment Type	From	To	Control Strategy	Graphical Record
1	Set Point Change in Top Products	x_{ov}: 0.7 x_{ss}: 0.53	0.65 0.45	PI + DC†	Figure 7, dashed lines
2	Set Point Change in Top Products	〃	〃	PI (parameters in Table 2)	Figure 7, solid lines
3	Set Point Change in Top Products	〃	〃	PI	Figure 8, solid lines
4	Set Point Change in Tray 19 Temp.	T_{19}: 92	97	PI + DC	Figure 10, dashed lines
5	Set Point Change in Tray 19 Temp.	T_{19}: 92	97	PI	Figure 10, solid lines
6	Set Point Change in Tray 19 Temp.	97	92	PI + DC	Figure 11, dashed lines
7	Set Point Change in Tray 19 Temp.	97	92	PI	Figure 11, solid lines
8	Disturbance in Feed Rate (Square pulse for	0.8 gpm	1.0 gm	PI + DC	Figure 12, dashed lines
9	Disturbance in Feed Rate one hour)	and return		PI	Figure 12, solid lines
10	Disturbance in Feed Temp.	78°	58°	PI + DC	Figure 14, dashed lines
11	Disturbance in Feed Temp.	78°	58°	PI	Figure 14, solid lines
12*	Set Point Change in Top Products	x_{ov}: 0.7 x_{22}: 0.5	0.65 0.42	PI + DC	Figure 16, dashed lines
13*	Set Point Change in Top Products	〃 〃	〃 〃	PI	Figure 16, solid lines
14*	Disturbance in Feed Rate	0.8 gpm (0.05 L/s)	1.0 gpm (0.06 L/s)	PI + DC	Figure 17, dashed lines
15*	Disturbance in Feed Rate	0.8 gpm (0.05 L/s)	1.0 gpm (0.06 L/s)	PI	Figure 17, solid lines

* Experimental runs under drastically altered operating conditions.
† Delay compensation.

LITERATURE CITED

Brookhaven National Laboratory, 1978 Estimates.

Freshwater, D. C., and E. Ziogou, "Reducing Energy Requirements in Unit Operations," *Chem. Eng. J.*, **11**, p. 215 (1976).

Lemaire, J. P., "Identification of a Distillation Column," MS Report, Univ. of Wisconsin, Madison (1980).

Mix, T. W., J. S. Dweck, and R. C. Armstrong, "The Potential for Energy Conservation in Distillation," Paper 87a, AIChE Annual Meeting (1977).

Ogunnaike, B. A., "Control Systems Design for Multivariable Systems with Multiple Time Delays," PhD Thesis, University of Wisconsin-Madison (1981).

Ogunnaike, B. A., and W. H. Ray, "Multivariable Controller Design for Linear Systems Having Multiple Time Delays," *AIChE J.*, **25**, p. 1043 (1979).

Ogunnaike, B. A., and W. H. Ray, "Computer-Aided Multivariable Control System Design for Processes with Time Delays," *Computers in Chemical Engineering* (1982).

Manuscript received October 15, 1981; revision received July 6, and accepted August 26, 1982.

Tracer Diffusion in Methanol, 1-Butanol and 1-Octanol from 298 to 433 K

Diffusion coefficients of argon, krypton, xenon, methane, carbon tetrachloride and the tetraalkyltins (methyl through butyl) were measured in methanol, 1-butanol and 1-octanol over the temperature range 298 to 433 K. With temperature-dependent solvent diameters fitted from the tracer diffusivity of one of the solutes, a rough-hard-sphere theory predicts well the observed tracer diffusivity over the solvent density range in which hard-sphere computer simulations are available. The Wilke-Chang correlation predicts diffusion coefficients in the higher alcohols with an average error of 80% and a maximum error of 200%. A correlation of the form $D\mu p/T = A$ where p and A depend on solute and solvent size is more successful giving an average error of 7% and a maximum error of 24%.

S.-H. CHEN, D. F. EVANS and H. T. DAVIS

Department Chemical Engineering and Materials Science University of Minnesota Minneapolis, MN 55455

SCOPE

There is as yet no adequate theory of tracer diffusion in alcohols and there is a dearth of experimental data at other than room temperature. This paper broadens the experimental data base to a wide range of temperatures (298 to 433 K) for argon, krypton, xenon, methane, carbon tetrachloride, and a series of tetraalkyltins (methyl through n-butyl) in methanol, 1-butanol and 1-octanol. A major aim of the paper is to extend to alcohols a rough-hard-sphere molecular theory and an empirical correlation scheme relating tracer diffusion, solvent viscosity and molecular sizes.